Heliyon 10 (2024) e36584

Contents lists available at ScienceDirect

Heliyon

journal homepage: www.cell.com/heliyon

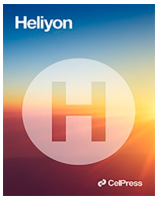

Research article

Effect of placental mesenchymal stem cells on promoting the healing of chronic burn wounds

Jinli Xiao [a,1], Qing Zhang [b,c,1], Bowen Wu [a], Maomao Wang [a], Yongzhao Zhu [d], Dan Zhao [c], Fang Zhao [c], Yan Xie [c,e,*]

[a] Clinical Medical School, Ningxia Medical University, Yinchuan, 750004, Ningxia, China
[b] Key Laboratory of Fertility Preservation and Maintenance of Ministry of Education, School of Basic Medical Sciences, Ningxia Medical University, Yinchuan, China
[c] Tissue Organ Bank & Tissue Engineering Centre, General Hospital of Ningxia Medical University, Yinchuan, 750004, Ningxia, China
[d] Surgery Lab, General Hospital of Ningxia Medical University, Yinchuan, 750004, Ningxia, China
[e] School of Biomedical Sciences, Faculty of Health, Queensland University of Technology, Brisbane, Australia

ARTICLE INFO

Keywords:
Chronic burn wounds
Placental mesenchymal stem cells
Fibroblasts
Keratinocytes
Wound healing

ABSTRACT

The treatment of chronic burn wounds is difficult in clinical practice. The ideal therapy is required to be continuously explored. Mesenchymal stem cells revolutionize the treatment of many diseases. The placental mesenchymal stem cells (PMSCs) have the characteristics of easy access, strong proliferation ability and multi-directional differentiation potential. The aim of this study was to investigate the potential of PMSCs in chronic burn wound healing. In this study, species of bacteria of 317 patients with chronic burn wounds have been analyzed. Samples of chronic burn wound fluid were collected from representative patients and then co-cultured with cells. In vitro studies showed that chronic burn wound fluid inhibited the proliferation of human keratinocytes and fibroblasts, while PMSCs can counteract the effects of burn wound fluid on inhibiting the proliferation and migration of human keratinocytes and fibroblasts. In addition, in vivo studies showed that a rat chronic burn wound model was successfully created. The expression of MMP-2, MMP-9, MDA, IL-6 and TNF-α in chronic burn wounds was significantly higher than that in acute burn wounds. Finally, the rat chronic burn wound model was used to verify that placental mesenchymal stem cell transplantation increased the wound healing rate, decreased the wound healing time, and promoted wound healing by increasing the thickness of epidermis and promoting the expression of P63 and CK10. The findings provide support for the hypothesis that PMSCs promote the repair of chronic burn wounds and key scientific data for the application of PMSCs as a new method for treating chronic burn wounds.

1. Introduction

Clinically, chronic burn wounds (CBW) are the wounds caused by severe burns [1,2]. And cannot restore structural and functional integrity through orderly and timely repair due to full-layer skin defects, long-term inflammation, bacterial invasion, granulation

* Corresponding author. Tissue Organ Bank & Tissue Engineering Centre, General Hospital of Ningxia Medical University, Yinchuan, 750004, Ningxia, China.
E-mail address: yanxie.yx@outlook.com (Y. Xie).
[1] These authors have contributed equally to this work.

https://doi.org/10.1016/j.heliyon.2024.e36584
Received 12 May 2024; Received in revised form 14 August 2024; Accepted 19 August 2024
Available online 22 August 2024

tissue maturity, bacterial biofilm, or new epithelium rupture [3]. Most chronic wounds have the characteristics of scattered wounds including tissue edema, severe immune inflammation injury, stagnant growth and poor wound margin epithelization. The wound does not heal for a long time after the formation of ulcers due to infection and uncontrollable wound changes [4]. The healing of burn wounds is a process of continuous tissue repair, and the basis of which is the activity of repair cells such as inflammatory cells, fibroblasts and endothelial cells [5,6]. These activities are affected by systemic and local factors. The repair time of CBW is longer and healing process is more difficult compared with normal wounds. The treatment of non-healing burn wounds is difficult in clinical practice, and it is also a research focus and difficulty in the field of burns. The ideal therapy is required to be continuously explored.

Stem cells revolutionize the treatment of many diseases [7–9]. The mesenchymal stem cells (MSCs) play a repairing role by releasing bioactive molecules through paracrine signaling signals, affecting cell migration, proliferation and survival of surrounding cells [10]. Placental mesenchymal stem cells (PMSCs) may be a suitable source for the treatment of chronic wounds base on the advantages of safe, stable proliferation and low immunogenicity [11]. The PMSCs can also be easily obtained from perinatal tissues and without invasive surgical and ethical problems [12]. It is reported that PMSCs have high proliferation and migration capabilities, especially under immediate hypoxic condition [13–16]. We therefore hypothesized that PMSCs may promote the healing of CBW.

2. Materials and methods

2.1. Ethic statements

The studies involving human participants were reviewed and approved by the Ethics Committee of the General Hospital of Ningxia Medical University (Ethical approval No. 2020–282). The CBWF collection approved by the Ethics Committee of the General Hospital of Ningxia Medical University (Ethical approval No. 2019–274). The participants provided their written informed consent to participate in this study. All methods were carried out in accordance with the declaration of Helsinki. The animal study was reviewed and approved by the Ethics Committee of the General Hospital of Ningxia Medical University (Ethical approval No. 2019–274) and treated in accordance with the Regulations for the administration of affairs concerning experimental animals (Ministry of Science and Technology, Beijing, China, revised in June 2004). All methods are reported in accordance with ARRIVE guidelines.

2.2. *Human chronic burn wound fluid (CBWF) collection [17–20]*

The information of patients with CBW were collected from January 2013 to March 2019 in the Department of Burns and Plastic Surgery. In this study, 317 patients of the Department of Burn and Plastic Surgery in the General Hospital of Ningxia Medical University between January 2013 and March 2019 with CBW were included. Samples of CBWF were collected from representative patients according to the inclusion and exclusion criteria in Table 1. The collected wound fluid was centrifuged at 5000g for 10 min and the filtered supernatant was stored at −80 °C. Bacterial identification were performed by VITEK2 Compact System (bioMérieux, Marcy-l'Étoile, France). Epidemiological statistical analysis of CBWF was performed on the basic information of patients and bacterial etiology.

2.3. Cell culture

All cells were cultured as previously reported [21–23]. Human fibroblasts (HFs) were isolated from skins from three different patients and cultured in 10 % fetal bovine serum (FBS; Biological industries, USA) medium under 5 % CO_2 and 37 °C, and the medium was changed every 3 days. The human keratinocytes (HKs) were provided by Concord Cell Resource Center and were cultured in MEM medium (Gibco, MA, USA). For PMSCs, cells were cultured in M8 medium (Lonza BioWhittaker, MD, USA) and kept at 37 °C with a minimum relative humidity of 95 % and an atmosphere of 5 % CO_2 in the air. All medium are free of antibiotics. Cells were dissociated and passaged by culture incubation with 0.05 % solution of trypsin-EDTA (Gibco, MA, USA) at a split ratio of 1:3 upon reaching 80–90 % confluency. Cells (passages 4–7) were used for experiments.

Table 1
Criteria for selecting patients.

	Inclusion criteria	Exclusion criteria
Completeness of medical records	Yes	No
Time	The wounds have not healed four weeks after the burn	Does not come up to the inclusion criteria
Age	Unlimited	None
Gender	Unlimited	None
Pathogen test	Positive	Negative
Disease	None	Pregnant or lactating women; patients with diabetes, pressure ulcers, immune diseases, vascular diseases, radiation damage, cancer, or severe infections; patients taking steroids and immunosuppressants; patients with allergies

2.3.1. Cells treated with CBWF

The wound fluid and cells were co-cultured to detect effects of CBWF on cells by Alamar Blue (AB) test (Sigma-Aldrich, MO, USA) and crystal violet (Sigma-Aldrich, MO, USA) [24]. The HKs at a concentration of 4×10^3 cells/100 μl were seeded onto 96-well plates (Eppendorf, MA, USA), while HFs were inoculated at a density of 3×10^3 cells/100 μl. After 12 h, CBWF was added separately. The positive groups were the cells cultured with MEM medium for HKs and 10 % FBS medium for HFs. The negative control group was the cells incubated with serum-free medium (SFM) from Gibco, CA, USA. After 48 h, plates were washed twice with PBS (Biological industries, CT, USA) and the optical density (OD) was measured in each group with AB test. The cells were then fixed with 4 % formalin (Biotopped, Beijing, China) for 20 min and stained with 0.1 % crystal violet to observe the changes in cell morphology. Cell proliferation rate= (OD value of experimental group)/(OD value of control group) x 100 %.

2.3.2. The co-cultivation system [25]

The groups of cells are shown in Fig. 1. In experimental group, 4×10^4 HK cells or 2×10^4 HF cells seeded onto the top chamber of Transwell (Millipore, MA, USA), with 6×10^4 PMSC cells seeded on the bottom chamber of the 48-well plate. In blank control group, 4×10^4 HK cells or 2×10^4 HF cells seeded onto the top chamber and SFM added to the bottom chamber of 48-well plate. In normal control group, 4×10^4 HK cells seeded on the top chamber and 6×10^4 HF cells seeded on the bottom chamber of the 48-well plate. After incubating overnight, the HK medium was changed to 300 μl CBWF, 600 μl SFM medium was added to the bottom chamber and the CBWF was incubated for 24 h. The SFM medium in the bottom chamber was then replaced with the medium corresponding to the cells to test cell migration and proliferation. None of the experiments has added antibiotics.

2.3.2.1. Transwell migration assay [26]. Transwell chamber with 8 μm membrane pore size was used to detect cell migration. The culture medium was removed after 24 h of incubation. Then, 200 μl 4 % formalin was added to each well for 20 min. Cells in the upper layer of the chamber were wiped off with a cotton swab, and the cells migrated under the chamber membrane were retained. The formalin was removed and 200 μl 0.1 % crystal violet was added, then incubated for 10 min. The plates were rinsed with tap water and dried overnight. Pictures were taken under low and high magnification microscopy (Olympus CX31, Tokyo, Japan). Acetic acid was added. After the well was dissolved, the absorbance was read with a 595 nm filter on Infinite 200 PRO series microplate reader (TECAN, Männedorf, Switzerland). Cell migration rate = (OD value of experimental group)/(OD value of control group) x 100 %.

2.3.2.2. Transwell proliferation assay [24]. Transwell chamber with 0.4 μm membrane pore size was used to detect cell proliferation. All cells on the chamber were calculated to indicate cell proliferation. The crystal violet treatments were same as cell migration mentioned before. Cell proliferation rate= (OD value of experimental group)/(OD value of control group) x 100 %.

2.3.3. Statistical analysis [27]

The three types of cells in all experiments were from three different patients and were tested three times in each single experiment. All measurement data used are expressed as the mean ± SEM. T-test was used to analyze whether there are statistical differences between groups with $P < 0.01$/$P < 0.05$ indicating that the differences between groups were statistically significant. GraphPad Prism version 7.0 (GraphPad Software Inc., CA, USA) was used to calculate the results and draw the graph.

2.4. Animal models

2.4.1. Creation of rat CBW models

The animal experiments were approved by The SPF female Sprague Dawley (SD) rats, 280–300 g in weight and 7–9 weeks of age

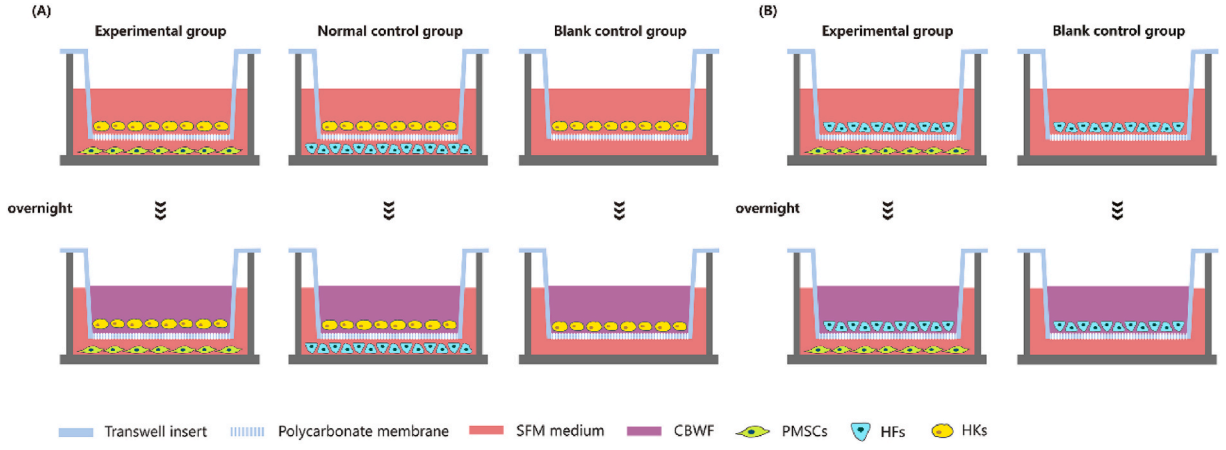

Fig. 1. Co-cultivation system. (A) HKs co-cultured with PMSCs. (B) HFs co-cultured with PMSCs.

were housed under conditions provided by the Animal Experiment Center of Ningxia Medical University. They were fasted overnight before the experiment and anesthetized with isoflurane (China National Medicines Corporation Ltd., Beijing, China), and then injected with 3 % sodium pentobarbital (Sigma-Aldrich, MO, USA) intraperitoneally. After anesthesia, the fur was clipped from the experimental operation site on the back of the mouse and depilatory cream was applied to the site topically. After 2–3 min, the remaining depilatory cream was washed with water and wiped with gauze. A surgical marker pen was used to mark a 2 cm circular scald area beside the midline of the rat's back. The scald time was set to 10 s, 15 s, 20 s, 25 s, 30 s, 35s. The burn temperature was set as 97 °C by a burn device (Yiyan Technology Development Co., Ltd., Beijing, China). After the operation, a circular full-thickness burn wound was created by the burn device which is acute burn wound (ABW). Epirubicin HCl (Meilunbio, Dalian, China) was then injected at 2 mg/ml within 0.2 cm of the edge of the ABW at five points with 60 μl/point to create CBW. Then, the rats were bandaged with an elastic bandage. SD rats were divided into 3 groups, including CBW (acute burn wounds injected with Epirubicin HCL), ABW (acute burn wounds) and Epirubicin HCL (Epirubicin HCL injection only). After 3, 7, 14, 21, and 28 days, the changes of wounds in each group were recorded and the tissues were collected for further analysis.

2.4.1.1. Wound healing assessment. For the animal models the Meeh-Rubner formula was used to calculate the total body surface area after a full-thickness burn in rats. Total Body Surface Area (TBSA) = S1/S S1 = $4 \times 3.14 \times 12 = 12.56\ cm^2$ [28]. S (Square) = $KW^{2/3}$ was used to calculate the surface area (cm^2), K represents the coefficient, and W represents the corresponding weight (g). S = $9.83 \times 2802/3\ cm^2 = 420.719\ cm^2$ and the trauma area ratio TBSA = $12.56\ cm^2/420.719\ cm^2 = 2.985$ %. Wounds were measured with a ruler, photographed with a digital camera and recorded at day 0, 3, 7, 14, 21 and 28. Digital image analysis software was used to analyze the wound area and the healing rate was calculated [29]. Wound healing rate= (original wound area-unhealed wound area)/original wound area × 100 %.

Hematoxylin-eosin (HE) staining was the gold standard for evaluating the morphology of burn [27]. Samples were burnt for 10 s, 15 s, 20 s, 25 s, 30 s, 35 s and then fixed and stained. The samples of Wounds in CBW, ABW and Epirubicin HCL groups at day 3, 7, 14, 21, and 28 days were also fixed and stained.

ELISA was used to detect the levels of superoxide dismutase (SOD), malondialdehyde (MDA), tumour necrosis factor-α (TNF-α) and Interleukin-6 (IL-6) in tissues after wounding. The skin tissues were washed, weighed, minced, and homogenized on ice in cold PBS. The homogenized mixtures were centrifuged at 3000rmp for 10 min at 4 °C. The supernatants were collected in 0.5 ml sterile tubes and stored at −80 °C prior to use. Homogenate tissue samples were prepared to determine SOD and MDA levels. The protein content of the homogenate was determined by BCA method. The absorbance was measured at 562 nm, and the protein concentration of each sample was calculated according to the standard curve. The SOD and MDA levels of tissue homogenate were detected according to the kit instructions (Nanjing Jiancheng bioengineering institute, Nanjing, China). The TNF-α and IL-6 levels were measured by enzyme-linked immunosorbent assay (ELISA) kits (Multi sciences, Hangzhou, China) according to the manufacturer's detailed instructions. The OD value at 450 nm was measured with a microplate reader, and the content (ng/L) of rat TNF-α and IL-6 in the samples was calculated.

The experimental method of immunohistochemistry (IHC) refers to the previous report [27]. Rat tissue sections were deparaffinized and rehydrated, following antigen retrieval with a citrate buffer. Slides were incubated with 3 % H_2O_2 at room temperature for 10 min to block endogenous peroxidase. Paraffin sections of 4 μm thickness were stained for matrix metalloproteinase-2 (MMP-2) (Servicebio, Wuhan, China), matrix metalloproteinase-9 (MMP-9) (Servicebio, Wuhan, China), SOD (Abmart, Shanghai, China) and MDA (Abmart, Shanghai, China). After incubating overnight at 4 °C in a humidity chamber box, the second antibody was added for 2h at room temperature. Finally, the slides were counterstained with hematoxylin solution, followed by dehydration and mounting.

2.4.2. Treatments

After the CBW models were successfully created, they were divided randomly as PMSC group, external recombinant human epidermal growth factor (GF) group (Gibco, CA, USA) and normal saline (NS) groups. For the PMSC group, 1×10^6 PMSCs were transplanted on the back of the rats every 3 days for 4 weeks. For the GF group, external recombinant human epidermal growth factor at 4000 IU/$10 \times 10\ cm^2$/wound was injected. And for the NS group, the same amount of physiological saline was injected. Wounds are observed and photted daily.

2.4.2.1. Wound healing assessment. HE staining and IHC have been undertaken as described above. The slides were stained for cytokeratin 10 (CK10) (Santa Cruz, TX, USA) and tumor protein 63 (P63) (Santa Cruz, TX, USA).

2.4.3. Statistical analysis

Image J (Rawak Software Inc., Stuttgart, Germany) was used to calculate the wound area of rats. An optical microscope (Olympus CX31, China) was adopted for the evaluation of the degree of staining for each image. The thickness of HE is measured by Image J and 3 random areas of 3 samples in each group were obtained (n = 9). Image-Pro plus 6.0 software (Media Cybernetics, MD, USA) was employed to quantify the immunohistochemical staining of protein expression. The integrated option density (IOD) value was obtained. Finally, the IOD of 3 random regions of 3 samples in each group was taken (n = 9). Comparisons among different groups were analyzed by Tukey's test. GraphPad Prism version 7.0 was used to calculate and plot the results.

3. Results

3.1. CBWF analysis

A total of 46 species of bacteria were discovered from CBWF of 317 patients of with CBW. The information related to the type, size, degree, and extent of burn wounds has been shown in Table 2. There are three types of burns, which are electrical burns, chemical burns, and thermal burns. The male accounted higher percentage of the population than the female, and the ratio of male to female was 5.34:1. The most common cause of injures was thermal burns as evidenced in 258 (81 %) patients, followed by electrical burns in 46 (15 %) and chemical burns in 13 (4 %). The patients were divided into four extent groups based on the TBSA and degree of burns including minor burns, moderate burns, severe burns and extra severe burns [30]. Assessment of the extent of burns revealed that 5 (2 %) patients had TBSA under 10 % or no third-degree burns. In addition, 189 (60 %) patients had TBSA between 11 % and 30 % or third-degree burns under 10 %. Moreover, 60 (19 %) patients had TBSA between 31 % and 50 % or third-degree burns of 10–19 %. Furthermore, 63 (20 %) patients with extra severe burns had TBSA more than 50 % or third-degree burns more than 20 %.

The top seven cultured bacteria were *staphylococcus aureus* (56.78 %), *coagulase-negative Staphylococcus* (18.30 %), *acinetobacter baumannii* (16.72 %), *enterobacter cloacae* (10.73 %), *methicillin-resistant staphylococcus aureus* (8.52 %), *pseudomonas aeruginosa* (7.26 %) and *kreber Pneumonia* (6 %) (Table 3). *Staphylococcus aureus* accounted for the largest proportion. The CBWF collected from patients infected by *staphylococcus aureus* were used to test the effect of PMSCs on CBW healing.

3.2. The effect of CBWF on HKs and HFs

After clinical collection of CBWF, they were co-cultured with HF and HK cells. After treatment, the spindle shape of HFs disappeared and the HKs scattered as small flakes (Fig. 2A), showing that the CBWF had the effect of inhibiting the growth of HKs and HFs compared with the control group. The AB assay showed that CBWF inhibited the proliferation of HKs, 30.41 % lower than the SFM group ($P < 0.01$) and 90.41 % lower than the MEM group ($P < 0.01$) (Fig. 2B). The CBWF inhibited the proliferation of HF, 27.8 % lower than the SFM group ($P < 0.01$) and 53.64 % lower than the 10 % FBS group ($P < 0.01$) (Fig. 2C). The CBWF inhibited the proliferation of HF, 27.8 % lower than the SFM group ($P < 0.01$) and 53.64 % lower than the 10 % FBS group ($P < 0.01$) (Fig. 2D). CBWF inhibited the proliferation of HKs and HFs.

3.3. Detecting the effects of PMSCs on cellular migration and proliferation

The CBWF was used to treat HFs and HKs to simulate the status of the pathological microenvironment of the CBW (Fig. 3A and B). The results showed that the migration of HKs promoted by PMSCs in the pathological microenvironment was 36.3 % higher than the HF group ($P < 0.01$), 65.6 % higher than the MEM group ($P < 0.01$) and 195.7 % higher than the SFM group ($P < 0.01$) (Fig. 3C). The migration of HFs promoted by PMSCs was 45.2 % higher than the 10 % FBS group ($P < 0.01$) and 95.2 % higher than the SFM group ($P < 0.01$) (Fig. 3D).

The proliferation of HKs promoted by PMSCs in the pathological microenvironment was 23.3 % higher than that of the HF group ($P < 0.01$), 54.1 % higher than that of the MEM group ($P < 0.01$) and 159.8 % higher than that of the SFM group ($P < 0.01$) (Fig. 3E). The PMSCs also promoted the proliferation of HFs in the pathological microenvironment, 31.2 % higher than the 10 % FBS group ($P < 0.01$) and 64.9 % higher than the SFM group ($P < 0.01$) (Fig. 3F). In summary, PMSCs promoted the migration and proliferation of HFs and HKs in the pathological microenvironment.

3.4. Creation of rat chronic burn models

Wounds were created from top to bottom beside the midline of the back of the rat. The set burn time was 10 s, 15 s, 20 s, 25 s, 30 s and 35 s. The burn temperature was 97 °C, and the control group is normal skin (Fig. 4A). After scalding, the center and edge tissues of the wound were taken for HE staining. The results are shown in Fig. 4B. The basal cell layer is not damaged after burn for 10 s and there are no blisters between the epidermis and the dermis, judged as a first-degree burn wound. The depth of burn for 15 s was similar to 10 s, with only the epidermal layer reduced and there was fluid leakage between the epidermis and the dermis. The epidermis fell off 20s after burn, classing it as a second-degree burn wound. The epidermis appeared necrotic and dermal collagen fractured 25 s after the scald, classing this as a second-degree burn wound. After a 30 s burn, the whole layer of the skin underwent coagulation necrosis and

Table 2
Features of burn wounds.

		Male	Female	Number of cases	Percentage (100 %)
Type of burns	Electrical burns	44	2	46	15 %
	Chemical burns	13	0	13	4 %
	Thermal burns	210	48	258	81 %
Extent of burns	Minor burns	4	1	5	2 %
	Moderate burns	156	33	189	60 %
	Severe burns	51	9	60	19 %
	Extra severe burns	56	7	63	20 %

Table 3
Proportion of bacteria in CBW.

Bacteria type	Cases	Proportion (%)
Staphylococcus aureus	180	56.78
Coagulase negative staphylococcus	58	18.30
Acinetobacter baumannii	53	16.72
Enterobacter cloacae	34	10.73
Methicillin-resistant staphylococcus aureus	27	8.52
Pseudomonas aeruginosa	23	7.26
Kreber pneumonia	19	6.00

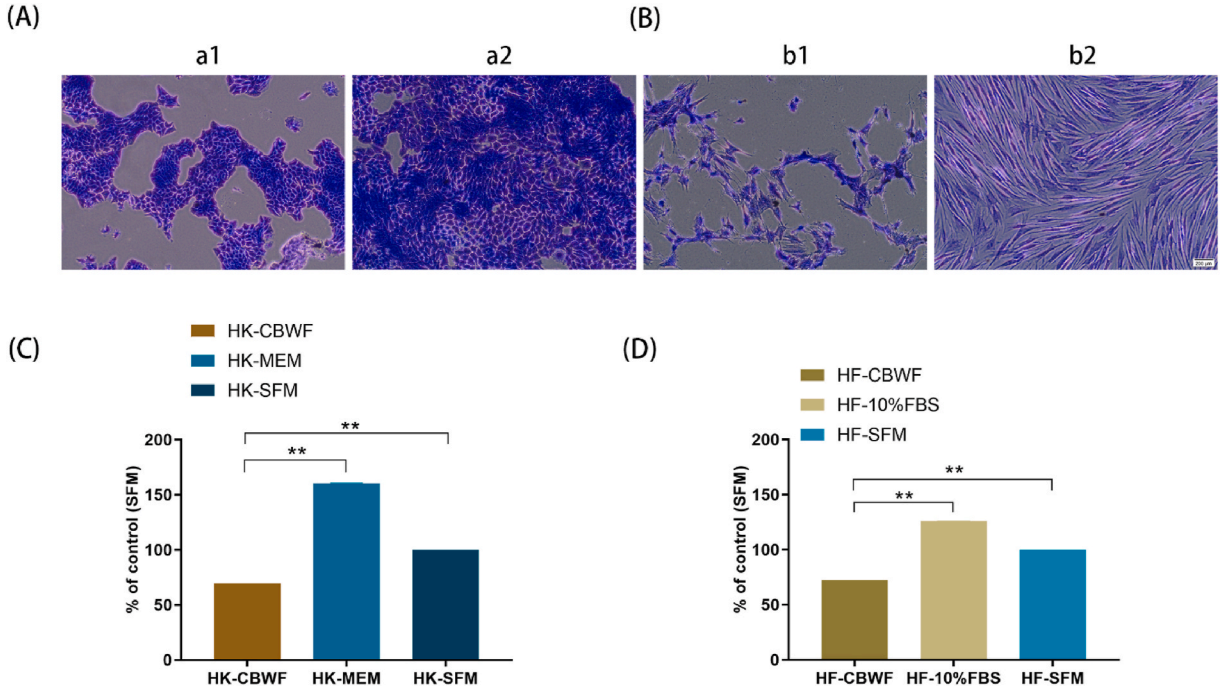

Fig. 2. (A) The effect of CBWF on HK morphology and viability (10X). (a1) Morphology of HKs treated with CBWF; (a2) HKs treated with control MEM medium. (B) The effect of CBWF on HF morphology and viability (10X). (b1) HFs treated with CBWF; (b2) HFs treated with control MEM medium. (C) Quantification of HK viability treated with CBWF. (D) Quantification of HF viability treated with CBWF. *P < 0.05 and **P < 0.01.

the whole layer of the dermis was broken and disordered, classing this as a third-degree burn wound. The burn depth of 35 s was like that of 30 s, with a large amount of exudate between the epidermis and the dermis. In addition, the epidermal cells of normal rat skin were arranged continuously. The nucleus and cytoplasm were clearly visible and the dermal layer and accessory structures were clear and complete. In conclusion, a burn of 30 s duration can lead to a full-thickness skin burn.

After the full-thickness skin burn was created, the Epirubicin HCl was injected at the edge of the wound to establish the rat CBW models. The experiment was divided into 3 groups, including CBW, ABW and Epirubicin HCL group. The wound healing was observed at day 3, 7, 14, 21 and 28 (Fig. 4C). On the 28th day, the wound area of CBW was still large and deep, and the inflammatory infiltration and epidermal crawling appeared. While most of the wounds in the ABW group and Epirubicin HCL group were covered with new epidermis. The new epidermis and stratum corneum were formed on the wound edge, and the subcutaneous collagen began to rebuild and arrange densely (Fig. 4D). Fig. 4F shows the wound healing rate CBW, ABW and Epirubicin HCL group at day 3, 7, 14, 21 and 28 respectively. In the ABW and Epirubicin HCL group, most of the wounds were epithelialized and healed, while the wounds in CBW group remained unhealed.

On the 28th day, Immunohistochemical results have shown that the expression of both MMP-2 and MMP-9 in CBW model was significantly higher than that in ABW and normal skin (Fig. 4E, K and 4L). The levels of SOD, MDA, TNF-α, IL-6 were estimated by ELISA to evaluate wound-healing progress (Table 4). The results revealed that the levels of MDA (Fig. 4G), TNF-α (Fig. 4I), IL-6 (Fig. 4J) significantly higher ($P < 0.01$) in CBW group compared with ABW group at day 3, 7, 14, 21and 28. By contrast, SOD (Fig. 4H) levels significantly lower ($P < 0.01$) in CBW compared with ABW group. These results are consistent with the study from IHC (Fig. 4M – P).

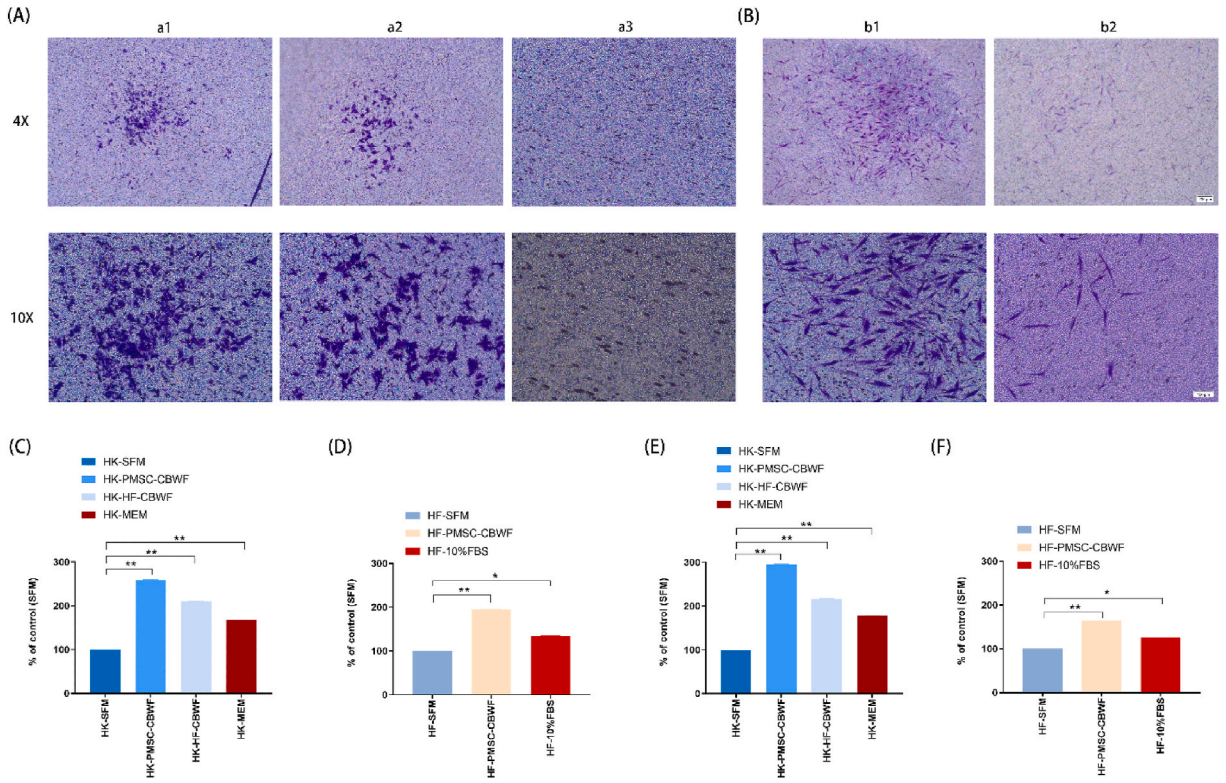

Fig. 3. PMSCs promote the migration and proliferation of HKs and HFs. (A) Morphology of HK (4X and 10X). a1) HKs co-cultured with PMSCs; a2) HKs co-cultured with HFs; a3) HKs cultured with SFM medium. (B) Morphology of HFs (4X and 10X). b1) HFs co-cultured with PMSCs; b2) HFs cultured with SFM medium. (C) Quantification of HK migration. (D) Quantification of HF migration. (E) Quantification of HK proliferation. (F) Quantification of HF proliferation. *P $<$ 0.05 and **P $<$ 0.01.

3.5. PMSCs transplantation promotes chronic wound healing

After the CBW model was established, the wounds were randomly divided into three groups as the PMSC, GF and NS group. The study found that wounds in the PMSC group healed after 18 days, wounds in the NS group healed after 30 days and wounds in the GF group healed after 20 days. Wounds in the PMSC group healed faster than the NS group and slightly faster than the GF group (Fig. 5A, D). Wound photographs were taken at day 4, 8, 12 and 16, and Image J software was used to calculate the area of the wound to obtain the wound healing rate (Fig. 5B and C). At day 4, 8, 12 and 16, the healing rate of the PMSC group gradually increased, at 28.96 % $\pm$ 2.54, 57.63 % $\pm$ 4.35, 79.15 % $\pm$ 3.85 and 91.25 % $\pm$ 1.87, respectively. The healing rate of CBW in the NS group gradually increased, at 19.43 % $\pm$ 3.55, 31.52 % $\pm$ 3.19, 46.35 % $\pm$ 3.81 and 47.72 % $\pm$ 5.99, respectively. The healing rage of CBW in the GF group was 44.29 % $\pm$ 3.96, 46.28 % $\pm$ 3.88, 62.47 % $\pm$ 4.48 and 77.81 % $\pm$ 2.62, respectively. Results showed that the wound healing rate of the PMSC group was higher than either GF group or NS group.

The thickness of the epidermis treated with both PMSC group and GF group were higher than that of the control group (P $<$ 0.01), and the difference in thickness between the two groups was not significant (P $>$ 0.05) (Fig. 6B). IHC was performed to evaluate expression of CK10 and P63 in rat from the three groups (Fig. 6A). At day 28, the positive staining of CK10 was strongly expressed in the PMSC group and GF group (P $<$ 0.05), and the positive staining of CK10 in the wounds treated with saline was significantly weak. There was no significant difference in the positive staining of CK10 between the PMSC group and the GF group. Fig. 6C shows that PMSCs can increase the expression of CK10 in the wound, followed by GF. The proliferation marker P63 is mainly expressed in the nucleus of proliferating keratinocytes. At day 28, the P63 staining of the wounds treated with saline was significantly lower than that of the wounds treated with PMSCs or GF (P $<$ 0.01). The expression of P63 in the PMSC group was slightly stronger than that in the GF group. Fig. 6D shows that PMSCs can increase the expression of P63 in wound healing. It can be concluded that PMSCs promote wound healing by increasing the thickness of epidermis and promoting the expression of P63 and CK10.

4. Discussion

The treatment of non-healing burn wounds is difficult in clinical practice, and the ideal therapy is required to be continuously explored. MSCs revolutionize the treatment of many diseases. Among them, PMSCs have the characteristics of easy access, low immunogenicity, strong proliferation ability and multi-directional differentiation potential [31]. This study hypothesized that PMSCs

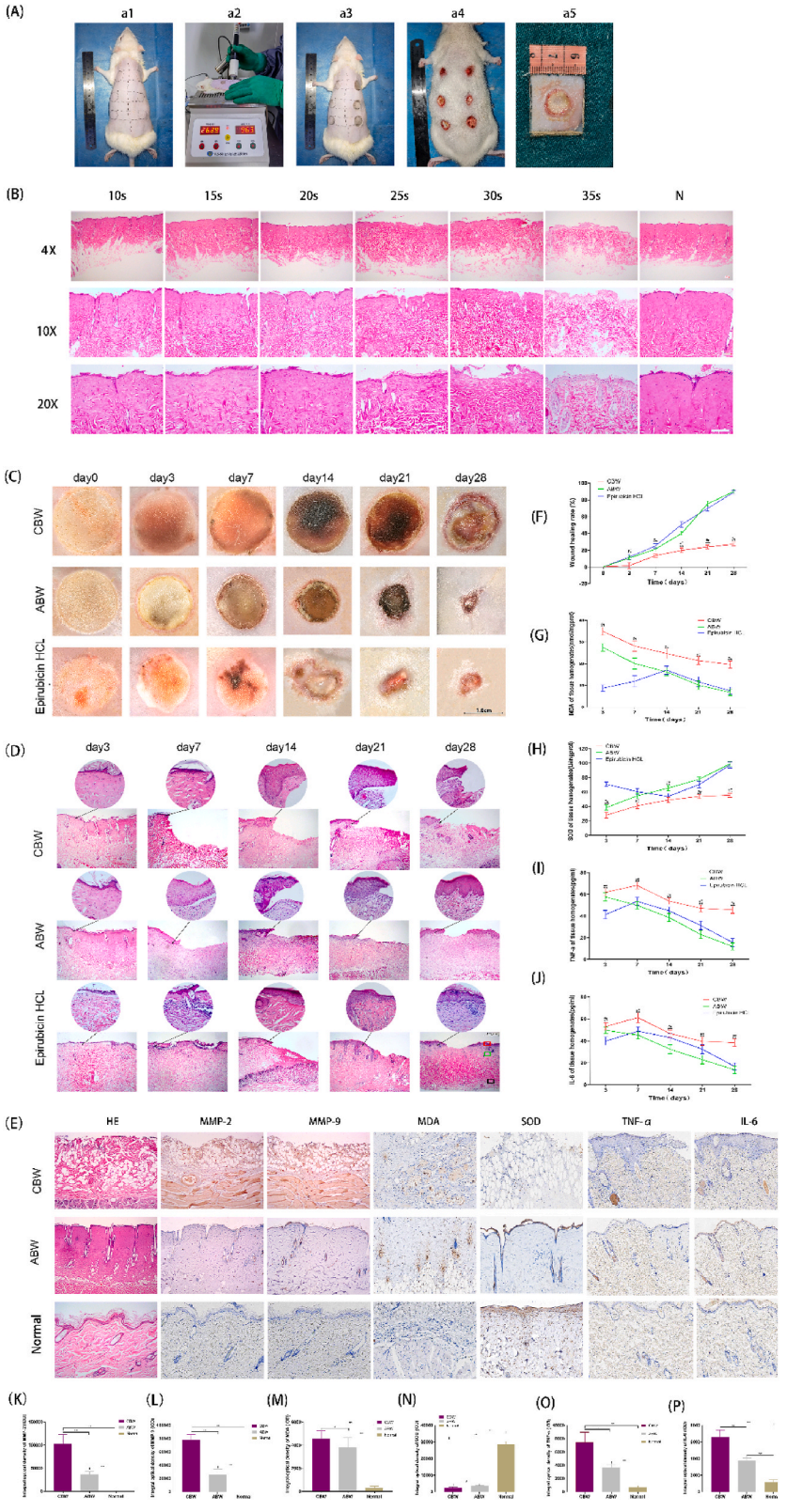

(caption on next page)

Fig. 4. (A) Establishment of an animal model of CBW. a1) The marked wounds; a2) The scalding process; a3) The ABW formed; a4) The CBW formed; a5) Enlarged view of the CBW. (B) The optimization of scald time. The burn time was set at 10 s, 15 s, 20 s, 25 s, 30 s and 35 s respectively (4X, 10X and 20X). N represents normal skin. (C) Outward appearance of three type of wounds (ABW, CBW and wounds treated with Epirubicin HCL) at day 0, 3, 7, 14, 21 and 28. (D) HE staining of wounds at day 3, 7, 14, 21 and 28 (4X and 20X). (E) HE staining (left) and IHC staining (right) of MMP-2, MMP-9, MDA, SOD, TNF-α and IL-6. (F) Quantification of the wound healing rate. Quantification of the MDA level (G), SOD level (H), TNF-α level (I), IL-6 level (J) (ELISA). Quantification of the MMP-2 (K), MMP-9 (L), MDA (M), SOD (N), TNF-α(O)and IL-6 (P) (immunohistochemistry). *P < 0.05, **P < 0.01.

can promote the repair of CBW.

In this study, species of bacteria of 317 patients with CBW have been analyzed. The most common causes of chronic wound infections is *staphylococcus aureus* (56.78 %), which is consistent with the study reported by Bess [32].

In order to mimic the micro-environment of BCW, CBWF was collected from representative patients and then co-cultured with cells. In vitro studies showed that CBWF inhibited the proliferation of HKs and HFs. The elevated levels of pro-inflammatory cytokines and matrix metalloproteinases (MMPs) in CWF lead to continuous self-digestion and degradation of the extracellular matrix (ECM) [33].

Importantly, we have found that PMCs can counteract the effects of burn wound fluid on inhibiting the proliferation and migration of HKs and HFs. The study undertaken by Kim et al. showed that adipose-derived MSCs promoted proliferation of HFs through paracrine pathways, reducing the wound area in vivo model significantly and promoted the re-epithelialization of the skin [34]. These findings were consistent with the results of this study. After PMSCs were co-cultured with HKs and HFs treated with CBWF, the proliferation and migration of these two cell types were improved. This may be due to the range of factors and exosomes secreted by PMSCs, which regulated the local environment of cells and stimulates cell proliferation, migration, survival and functional recovery [35]. Also, results showed that HFs can promote the proliferation and migration of HK treated with CBWF. HFs can secrete a variety of growth factors through autocrine and paracrine methods. Among these, keratinocyte growth factor is a specific growth factor that promotes the proliferation, differentiation and migration of HKs. It is weakly expressed in normal skin, but are expressed in enormous quantities in the process of tissue damage and repair [36].

Cell models cannot completely simulate the complexity of pathological damage in vivo, so animal models have been applied [37]. Chronic wounds are caused by the interruption of continuous links in the process of wound healing. The formation mechanism of chronic wounds is complicated. In recent years, many models have been established to study the formation mechanism of chronic wounds, including ischemia, diabetes, pressure and reperfusion injury, however, the above wounds have not lasted for four weeks [38,39]. In this study, a rat CBW model was created and the wounds have lasted for over 4 weeks. The microenvironment/physiology of created acute and chronic wounds at day 3, 7, 14, 21 and 28 days have been examined and illustrated in Fig. 4. Results have shown that the levels of MDA, TNF-α, IL-6, MMP-2 and MMP-9 are significantly higher in CBW group compared with ABW group ($P < 0.05$); while the level of SOD in CBW group is significantly lower than the ABW group ($P < 0.05$). Importantly, the expression of both MMP-2 and MMP-9 in CBW was significantly higher than that in acute burn wounds. In our models, there was no epidermal growth on the wound after the scab was lifted, which was similar in appearance to the clinically chronic wounds. MMP-2 (gelatinase A) and MMP-9 (gelatinase B) are metallogelatinases that have been extensively studied during cell migration and re-epithelialization [40]. They play a major role in physiological tissue remodeling processes such as organogenesis and wound healing [41]. The MMP-2 and MMP-9 in the CBWF remain high level, which can be used to display the condition of the wound and predict wound healing status [42,43]. In addition, reactive oxygen species (ROS) are key to wound healing. Excessive ROS can cause oxidative stress, resulting in damage to proteins, lipids and DNA in different cells, leading to prolongation and worsening of inflammatory processes, detrimental to wound healing and hindering the formation of new tissue [44]. The MDA level is an indirect measure of free radical activity as an indicator of oxidative stress. MDA levels indicate the damage level of tissue cell [45]. Our results showed that Epirubicin HCl increased the SOD activities in the healing wounds, thereby significantly decreasing MDA level. Our results identified multiple signs of oxidative stress in chronic wounds with significant differences. The high expression of inflammatory cytokines TNF-α and IL-6 in chronic wounds verified the inflammatory environment of wounds. Due to high levels of MMPs are associated with the formation of chronic wound [43], inflammation and the oxidative stress, the CBW model was established effectively.

In vivo studies showed that a rat CBW model was successfully created. The expression of MMP-2, MMP-9, MDA, IL-6 and TNF-α in CBW was significantly higher than that in acute burn wounds. The rat CBW model was then used to verify that PMSCs enhance CBW healing.

Delayed healing of burn wounds will increase the patient's susceptibility to infection, prolong pain, increase surgical procedures, increase the incidence of hypertrophic scars, and extend the length of hospital stay. Stem cell therapy may reduce these incidences [46]. However, it has been reported that the direct implantation of MSCs into the injured site leads to poor survival [47]. In this study, PMSCs were transplanted five mm outside the wound. This area has less inflammation and rich blood supply, which is conducive to the survival of PMSCs. Relevant studies have confirmed that PMSCs can accelerate wounds by reducing pro-inflammatory factors, enhancing the ability of wound immune cells, stimulating the proliferation of endothelial cells to promote blood vessel production and regulating the survival and proliferation of HFs and HKs [48,49]. The PMSC group and GF group of IHC had significantly higher P63 and CK10 expression than the NS group (Fig. 6A), indicating that PMSCs can promote cell proliferation and differentiation. In addition, this experiment found that when PMSCs repair wounds, there is a significant effect in the late stage rather than the early stage of wound healing. It is considered that the comprehensive effect of mesenchymal stem cells on chronic wounds can be further exerted after the survival of local transplantation of PMSCs.

Table 4
Comparison of wounds in ABW, CBW, Epirubicin HCL groups at day 3, 7, 14, 21 and 28 (ELISA).

	Wound healing rate(%)			MDA(nmol/mg)			SOD(u/mg)			TNF- α(pg/ml)			IL-6 (pg/ml)		
	CBW	ABW	Epirubicin HCL	CBW	ABW	Epirubicin HCL	CBW	ABW	Epirubicin HCL	CBW	ABW	Epirubicin HCL	CBW	ABW	Epirubicin HCL
Day 3	1.5 ± 3.8	10.5 ± 2.3	11.8 ± 3.2	34.9 ± 1.9	27.6 ± 1.8	8.8 ± 1.5	28.0 ± 4.0	38.4 ± 3.7	70.6 ± 3.3	61.9 ± 3.4	57.7 ± 3.8	41.2 ± 3.8	53.1 ± 3.5	49.5 ± 3.1	39.8 ± 3.8
Day 7	13.4 ± 2.3	21.2 ± 2.6	25.0 ± 2.8	28.2 ± 2.4	20.1 ± 2.6	11.9 ± 2.7	40.8 ± 3.8	54.6 ± 3.8	60.4 ± 4.3	68.2 ± 3.1	49.8 ± 3.5	53.5 ± 3.6	61.1 ± 4.4	45.2 ± 3.6	48.8 ± 3.8
Day 14	19.7 ± 2.8	39.8 ± 1.8	50.4 ± 3.5	24.7 ± 2.3	16.2 ± 1.8	17.1 ± 1.9	48.7 ± 3.6	65.2 ± 3.9	53.9 ± 4.1	53.8 ± 2.9	38.6 ± 3.7	44.8 ± 3.4	46.5 ± 3.2	32.3 ± 4.1	42.8 ± 3.5
Day 21	23.8 ± 2.3	75.2 ± 2.5	69.8 ± 3.4	21.4 ± 1.8	10.2 ± 2.0	11.6 ± 2.3	53.8 ± 2.9	77.7 ± 3.3	70.2 ± 4.6	47.1 ± 3.1	22.9 ± 3.7	31.3 ± 3.9	39.5 ± 3.9	22.7 ± 3.9	32.2 ± 4.1
Day 28	27.1 ± 2.1	89.7 ± 2.5	88.7 ± 2.4	19.6 ± 1.7	6.8 ± 1.5	7.6 ± 1.6	55.5 ± 3.1	98.8 ± 3.2	97.3 ± 4.0	45.6 ± 3.3	11.8 ± 3.2	15.5 ± 3.7	38.3 ± 3.4	13.5 ± 3.5	16.5 ± 3.2

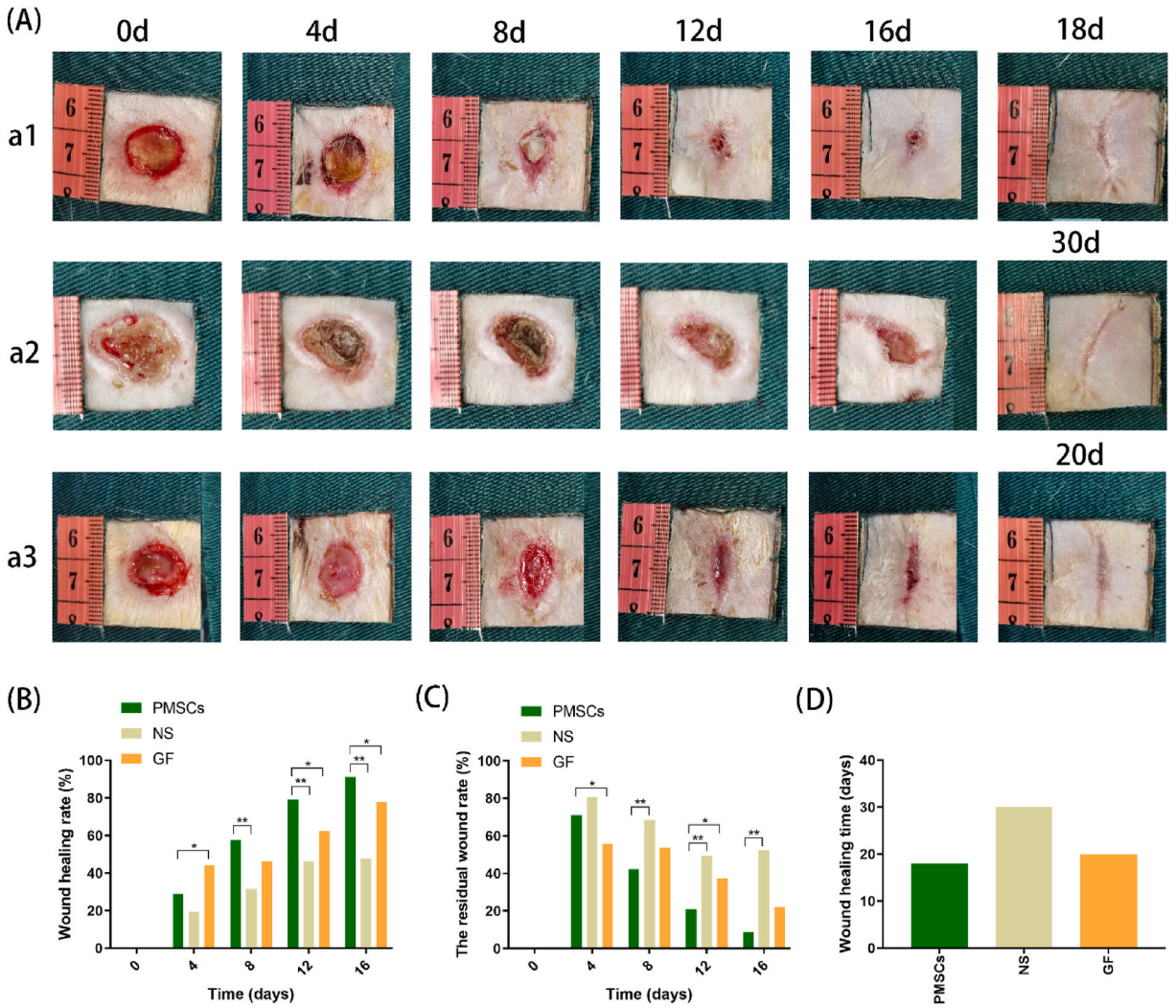

Fig. 5. PMSCs increased CBW healing. (A) CBW were treated with PMSC (a1), NS (a2) and GF (a3) at day 0, 4, 8, 12, 16, 18, 20 and 30. (B) Quantification of the wound healing rate. (C) Quantification of the wound residual rate. (D) Quantification of the wound healing time. *P < 0.05, **P < 0.01.

5. Conclusion

In vitro studies showed that CBWF inhibited the proliferation of human keratinocytes and fibroblasts, while PMSCs can counteract the effects of CBWF on inhibiting the proliferation and migration of HKs and HFs. In addition, in vivo studies showed that a rat CBW model was successfully created. The results have shown that transplantation of PMSCs increased the wound healing rate and decreased the wound healing time. In summary, PMSCs promote the repair of chronic burn wounds.

Institutional review board statement

The animal study was reviewed and approved by the Ethics Committee of the General Hospital of Ningxia Medical University (Ethical approval No. 2019–274).

Disclosure statement

No competing financial interests exist.

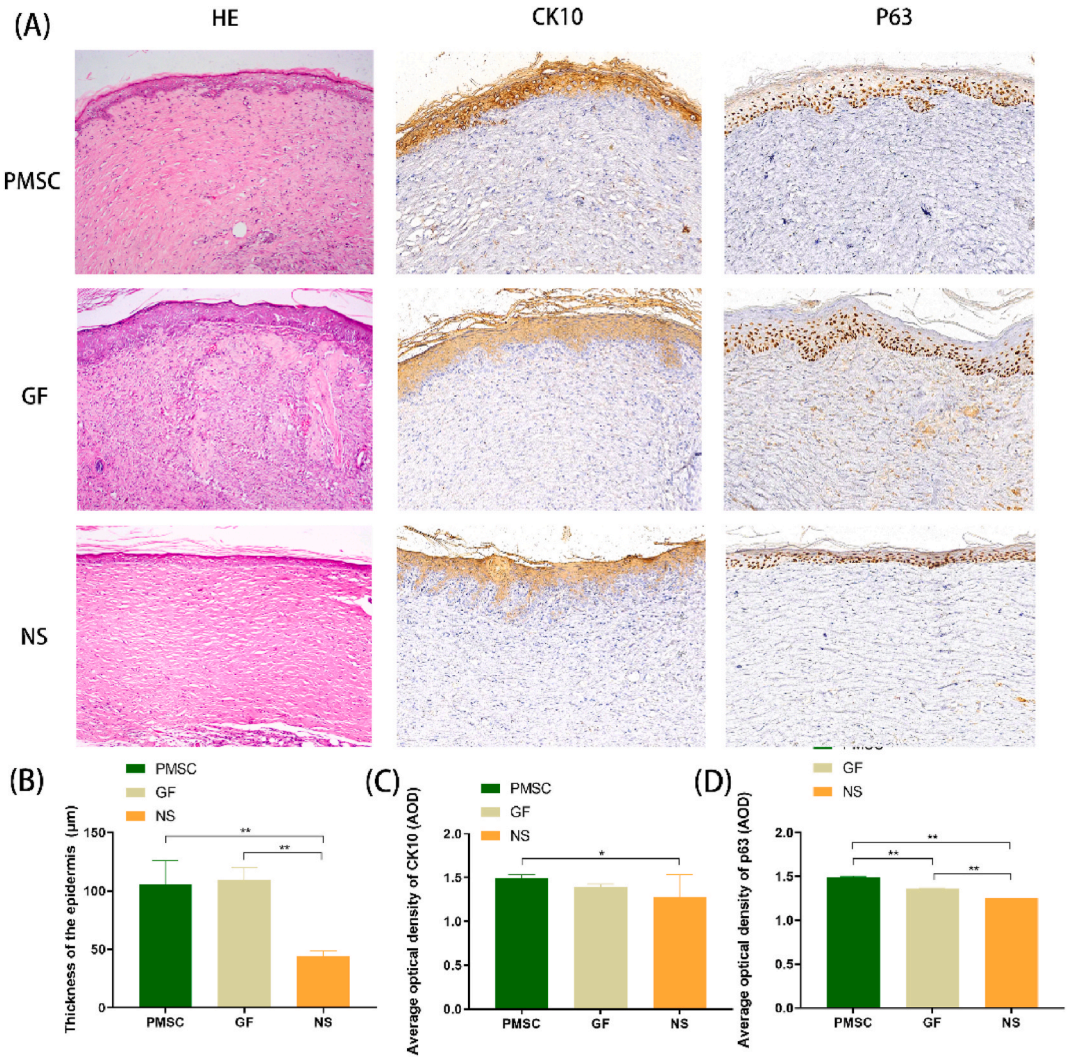

Fig. 6. Histologic and immunohistochemical analysis of the effects of PMSCs on CBW. (A) HE stain image and IHC analysis of CK10, P63 of regenerated skin tissue at day 28 post-treatment with MSC (n = 9), GF (n = 9) and saline (n = 9) (10X) (B) Quantification of epidermal thickness. (C) Quantification of CK10 staining. (D) Quantification of P63 staining. Differences with values of $P < 0.05$ were considered statistically significant. *$P < 0.05$, **$P < 0.01$. Error bars indicate SEM. Scale bar = 100 μm.

Funding

This study was supported by Science and Technology Department of Ningxia Hui Autonomous Region, China ; Key Research and Development Plan of Ningxia Hui Autonomous Region, China.

Data availability statement

The relevant data can be obtained from the corresponding author upon reasonable request.

CRediT authorship contribution statement

Jinli Xiao: Writing – original draft, Methodology, Formal analysis, Data curation. **Qing Zhang:** Writing – review & editing, Writing – original draft, Supervision, Data curation. **Bowen Wu:** Methodology. **Maomao Wang:** Methodology. **Yongzhao Zhu:** Supervision. **Dan Zhao:** Data curation. **Fang Zhao:** Data curation. **Yan Xie:** Writing – review & editing, Supervision, Project administration, Conceptualization.

Declaration of competing interest

The authors declare that they have no known competing financial interests or personal relationships that could have appeared to influence the work reported in this paper.

Acknowledgments

We thank Dr. Nanxiong Chen and Chao Fang for collecting CBWF. We also thank International Science Editing (http://www.internationalscienceediting.com) for editing this manuscript.

References

[1] M.C. Mauck, C.E. Barton, A. Tungate, J.W. Shupp, R. Karlnoski, D.J. Smith, F.N. Williams, S.W. Jones, K.V. McGrath, B.A. Cairns, S.A. McLean, Peritraumatic vitamin D levels predict chronic pain severity and contribute to racial differences in pain outcomes following major thermal burn injury, J. Burn Care Res. 42 (6) (2021) 1186–1191, https://doi.org/10.1093/jbcr/irab031.
[2] S.T. Elkins-Williams, W.A. Marston, C.S. Hultman, Management of the chronic burn wound, Clin. Plast. Surg. 44 (3) (2017) 679–687, https://doi.org/10.1016/j.cps.2017.02.024.
[3] G.S. Lazarus, D.M. Cooper, D.R. Knighton, D.J. Margolis, R.E. Percoraro, G. Rodeheaver, M.C. Robson, Definitions and guidelines for assessment of wounds and evaluation of healing, Wound Repair Regen. 2 (3) (1994) 165–170, https://doi.org/10.1046/j.1524-475x.1994.20305.x.
[4] R.G. Frykberg, J. Banks, Challenges in the treatment of chronic wounds, Adv. Wound Care 4 (9) (2015) 560–582, https://doi.org/10.1089/wound.2015.0635.
[5] Y. Wang, J. Beekman, J. Hew, S. Jackson, A.C. Issler-Fisher, R. Parungao, S.S. Lajevardi, Z. Li, P.K.M. Maitz Burn injury, Challenges and advances in burn wound healing, infection, pain and scarring, Adv. Drug Deliv. Rev. 123 (2018) 3–17, https://doi.org/10.1016/j.addr.2017.09.018.
[6] C.I. Schulman, N. Namias, L. Pizano, L. Rodriguez-Menocal, D. Aickara, W. Guzman, A. Candanedo, E. Maranda, A. Beirn, E.V. Badiavas, The effect of mesenchymal stem cells improves the healing of burn wounds: a phase 1 dose-escalation clinical trial, Scars Burn Heal 8 (2022) 205951312110707, https://doi.org/10.1177/20595131211070783.
[7] W. Zakrzewski, M. Dobrzyński, M. Szymonowicz, Z. Rybak, Stem cells: past, present, and future, Stem Cell Res. Ther. 10 (1) (2019) 68, https://doi.org/10.1186/s13287-019-1165-5.
[8] H.M. Blau, G. Q, DaleyStem cells in the treatment of disease, N. Engl. J. Med. 380 (18) (2019) 1748–1760, https://doi.org/10.1056/nejmra1716145.
[9] A.O. Lukomskyj, N. Rao, L. Yan, J.S. Pye, H. Li, B. Wang, J.J. Li, Stem cell-based tissue engineering for the treatment of burn wounds: a systematic review of preclinical studies, Stem Cell Rev Rep 18 (6) (2022) 1926–1955, https://doi.org/10.1007/s12015-022-10341-z.
[10] S. Maxson, E.A. Lopez, D. Yoo, A. Danilkovitch-Miagkova, M.A. LeRoux, Concise review: role of mesenchymal stem cells in wound repair, Stem Cells Transl Med 1 (2) (2012) 142–149, https://doi.org/10.5966/sctm.2011-0018.
[11] A. Shehadah, J. Chen, A. Pal, S. He, A. Zeitlin, X. Cui, A. Zacharek, Y. Cui, C. Roberts, M. Lu, R. Hariri, M. Chopp, Human placenta-derived adherent cell treatment of experimental stroke promotes functional recovery after stroke in young adult and older rats, PLoS One 9 (1) (2014) e86621, https://doi.org/10.1371/journal.pone.0086621.
[12] R. Hass, C. Kasper, S. Böhm, R. Jacobs, Different populations and sources of human mesenchymal stem cells (MSC): a comparison of adult and neonatal tissue-derived MSC, Cell Commun. Signal. 9 (1) (2011) 12, https://doi.org/10.1186/1478-811x-9-12.
[13] S. Barlow, G. Brooke, K. Chatterjee, G. Price, R. Pelekanos, T. Rossetti, M. Doody, D. Venter, S. Pain, K. Gilshenan, K. Atkinson, Comparison of human placenta- and bone marrow–derived multipotent mesenchymal stem cells, Stem Cell. Dev. 17 (6) (2008) 1095–1108, https://doi.org/10.1089/scd.2007.0154.
[14] P.S. in 't Anker, S.A. Scherjon, C.K.D. Keur, G.M.J.S. De Groot-Swings, F.H.J. Claas, W.E. Fibbe, H.H.H. Kanhai, Isolation of mesenchymal stem cells of fetal or maternal origin from human placenta, Stem Cell. 22 (7) (2004) 1338–1345, https://doi.org/10.1634/stemcells.2004-0058.
[15] G. Brooke, H. Tong, J.-P. Levesque, K. Atkinson, Molecular trafficking mechanisms of multipotent mesenchymal stem cells derived from human bone marrow and placenta, Stem Cell. Dev. 17 (5) (2008) 929–940, https://doi.org/10.1089/scd.2007.0156.
[16] Y. Wu, R.C.H. Zhao, E.E. Tredget, Concise review: bone marrow-derived stem/progenitor cells in cutaneous repair and regeneration, Stem Cell. 28 (5) (2010) 905–915, https://doi.org/10.1002/stem.420.
[17] A. Junka, W. Wojtowicz, A. Ząbek, G. Krasowski, D. Smutnicka, B. Bakalorz, A. Boruta, M. Dziadas, P. Młynarz, P.P. Sedghizadeh, M. Bartoszewicz, Metabolic profiles of exudates from chronic leg ulcerations, J. Pharm. Biomed. Anal. 137 (2017) 13–22, https://doi.org/10.1016/j.jpba.2017.01.018.
[18] R. Papa-Ezdra, L. Caiata, R. Palacio, M. Outeda, L. Cabezas, A. Bálsamo, R. Vignoli, I. Bado, V. Seija, Prevalence and molecular characterisation of carbapenemase-producing Enterobacterales in an outbreak-free setting in a single hospital in Uruguay, J Glob Antimicrob Resist 24 (2021) 58–62, https://doi.org/10.1016/j.jgar.2020.11.006.
[19] Y. Xie, S.C. Rizzi, R. Dawson, E. Lynam, S. Richards, D.I. Leavesley, Z. Upton, Development of a Three-Dimensional human skin equivalent wound model for investigating novel wound healing therapies, Tissue Eng. C Methods 16 (5) (2010) 1111–1123, https://doi.org/10.1089/ten.tec.2009.0725.
[20] M. Wu, Y. Li, D. Guo, G. Kui, B. Li, Y. Deng, F. Li, Microbial diversity of chronic wound and successful management of traditional Chinese medicine, Evid Based Complement Alternat Med 2018 (2018) 1–13, https://doi.org/10.1155/2018/9463295.
[21] Y. Zhu, X. Song, J. Wang, Y. Li, Y. Yang, T. Yang, H. Ma, L. Wang, G. Zhang, W.C. Cho, X. Liu, J. Wei, Placental mesenchymal stem cells of fetal origin deposit epigenetic alterations during long-term culture under serum-free condition, Expet Opin. Biol. Ther. 15 (2) (2014) 163–180, https://doi.org/10.1517/14712598.2015.960837.
[22] Y. Zhu, Y. Yang, Y. Zhang, G. Hao, T. Liu, L. Wang, T. Yang, Q. Wang, G. Zhang, J. Wei, Y. Li, Placental mesenchymal stem cells of fetal and maternal origins demonstrate different therapeutic potentials, Stem Cell Res. Ther. 5 (2) (2014) 48, https://doi.org/10.1186/scrt436.
[23] Q. Chen, H. Zhou, Y. Yang, M. Chi, N. Xie, H. Zhang, X. Deng, D. Leavesley, H. Shi, Y. Xie, Investigating the potential of Oxymatrine as a psoriasis therapy, Chem. Biol. Interact. 271 (2017) 59–66, https://doi.org/10.1016/j.cbi.2017.04.020.
[24] L. Rodriguez-Menocal, M. Salgado, D. Ford, E. Van Badiavas, Stimulation of skin and wound fibroblast migration by mesenchymal stem cells derived from normal donors and chronic wound patients, Stem Cells Transl Med 1 (3) (2012) 221–229, https://doi.org/10.5966/sctm.2011-0029.
[25] Z. Wang, Y. Wang, F. Farhangfar, M. Zimmer, Y. Zhang, Enhanced keratinocyte proliferation and migration in Co-culture with fibroblasts, PLoS One 7 (7) (2012) e40951, https://doi.org/10.1371/journal.pone.0040951.
[26] D. Lü, X. Liu, Y. Gao, B. Huo, Y. Kang, J. Chen, S. Sun, L. Chen, X. Luo, M. Long, Asymmetric migration of human keratinocytes under mechanical stretch and cocultured fibroblasts in a wound repair model, PLoS One 8 (9) (2013) e74563, https://doi.org/10.1371/journal.pone.0074563.
[27] X. Deng, Q. Chen, L. Qiang, M. Chi, N. Xie, Y. Wu, M. Yao, D. Zhao, J. Ma, N. Zhang, Y. Xie, Development of a Porcine Full-Thickness Burn Hypertrophic scar model and investigation of the effects of Shikonin on hypertrophic scar remediation, Front. Pharmacol. 9 (2018) 590, https://doi.org/10.3389/fphar.2018.00590.
[28] K.D. Capek, L.E. Sousse, G. Hundeshagen, C.D. Voigt, O.E. Suman, C.C. Finnerty, K. Jennings, D.N. Herndon, Contemporary burn survival, J. Am. Coll. Surg. 226 (4) (2018) 453–463, https://doi.org/10.1016/j.jamcollsurg.2017.12.045.
[29] E. Gouma, Y. Simos, I. Verginadis, E. Lykoudis, A. Evangelou, S. Karkabounas, A simple procedure for estimation of total body surface area and determination of a new value of Meeh's constant in rats, Lab. Anim 46 (1) (2012) 40–45, https://doi.org/10.1258/la.2011.011021.
[30] M. Yu, Q. Lv, H. Ding, X. Zeng, J. Cao, J. Liu, H. Fan, S. Hou, Evaluation of blast injury patients from the 2015 Tianjin explosions in China, Burns 42 (5) (2016) 1133–1140, https://doi.org/10.1016/j.burns.2016.03.004.

[31] J. Lu, Z. Liu, M. Shu, L. Zhang, W. Xia, L. Tang, J. Li, B. Huang, H. Li, Human placental mesenchymal stem cells ameliorate chemotherapy-induced damage in the testis by reducing apoptosis/oxidative stress and promoting autophagy, Stem Cell Res. Ther. 12 (1) (2021) 199, https://doi.org/10.1186/s13287-021-02275-z.
[32] L.J. Bessa, P. Fazii, M. Di Giulio, L. Cellini, Bacterial isolates from infected wounds and their antibiotic susceptibility pattern: some remarks about wound infection, Int. Wound J. 12 (1) (2013) 47–52, https://doi.org/10.1111/iwj.12049.
[33] C. Wiegand, U. Schönfelder, M. Abel, P. Ruth, M. Kaatz, U.-C. Hipler, Protease and pro-inflammatory cytokine concentrations are elevated in chronic compared to acute wounds and can be modulated by collagen type I in vitro, Arch. Dermatol. Res. 302 (6) (2009) 419–428, https://doi.org/10.1007/s00403-009-1011-1.
[34] W.S. Kim, B.S. Park, J.H. Sung, J.M. Yang, S.B. Park, S.J. Kwak, J.S. Park, Wound healing effect of adipose-derived stem cells: a critical role of secretory factors on human dermal fibroblasts, J. Dermatol. Sci. 48 (1) (2007) 15–24, https://doi.org/10.1016/j.jdermsci.2007.05.018.
[35] C. Salomon, J. Ryan, L. Sobrevia, M. Kobayashi, K. Ashman, M. Mitchell, G.E. Rice, Exosomal signaling during hypoxia mediates microvascular endothelial cell migration and vasculogenesis, PLoS One 8 (7) (2013) e68451, https://doi.org/10.1371/journal.pone.0068451.
[36] S. Werner, Keratinocyte growth factor: a unique player in epithelial repair processes, Cytokine Growth Factor Rev. 9 (2) (1998) 153–165, https://doi.org/10.1016/s1359-6101(98)00010-0.
[37] A. Abdullahi, S. Amini-Nik, M.G. Jeschke, Animal models in burn research, Cell. Mol. Life Sci. 71 (17) (2014) 3241–3255, https://doi.org/10.1007/s00018-014-1612-5.
[38] R. Nunan, K.G. Harding, P. Martin, Clinical challenges of chronic wounds: searching for an optimal animal model to recapitulate their complexity, Dis Model Mech 7 (11) (2014) 1205–1213, https://doi.org/10.1242/dmm.016782.
[39] C.D. Tipton, N.E. Sanford, J.A. Everett, R.A. Gabrilska, R.D. Wolcott, K.P. Rumbaugh, C.D. Phillips, Chronic wound microbiome colonization on mouse model following cryogenic preservation, PLoS One 14 (8) (2019) e0221565, https://doi.org/10.1371/journal.pone.0221565.
[40] M.G. Rohani, W.C. Parks, Matrix remodeling by MMPs during wound repair, Matrix Biol. 44–46 (2015) 113–121, https://doi.org/10.1016/j.matbio.2015.03.002.
[41] L. Ravanti, V.M. Kähäri, Matrix metalloproteinases in wound repair, Int. J. Mol. Med. 6 (4) (2000) 391–407, https://doi.org/10.3892/ijmm.6.4.391.
[42] A.B. Wysocki, L. Staiano-Coico, F. Grinnell, Wound fluid from chronic leg ulcers contains elevated levels of metalloproteinases MMP-2 and MMP-9, J. Invest. Dermatol. 101 (1) (1993) 64–68, https://doi.org/10.1111/1523-1747.ep12359590.
[43] A. Tardáguila-García, E. García-Morales, J.M. García-Alamino, F.J. Álvaro-Afonso, R.J. Molines-Barroso, J.L. Lázaro-Martínez, Metalloproteinases in chronic and acute wounds: a systematic review and meta-analysis, Wound Repair Regen. 27 (4) (2019) 415–420, https://doi.org/10.1111/wrr.12717.
[44] U.A.D. Keller, A. Kümin, S. Braun, S. Werner, Reactive oxygen species and their detoxification in healing skin wounds, J. Invest. Dermatol. Symp. Proc. 11 (1) (2006) 106–111, https://doi.org/10.1038/sj.jidsymp.5650001.
[45] J. Wang, J. Wang, G. Wang, L. Zhu, J. Wang, DNA damage and oxidative stress induced by imidacloprid exposure in the earthworm Eisenia fetida, Chemosphere 144 (2016) 510–517, https://doi.org/10.1016/j.chemosphere.2015.09.004.
[46] C. Bojanic, K. To, A. Hatoum, J. Shea, K.T.M. Seah, W. Khan, C.M. Malata, Mesenchymal stem cell therapy in hypertrophic and keloid scars, Cell Tissue Res. 383 (3) (2021) 915–930, https://doi.org/10.1007/s00441-020-03361-z.
[47] M. Li, Y. Zhao, H. Hao, W. Han, X. Fu, Mesenchymal stem cell–based therapy for nonhealing wounds: today and tomorrow, Wound Repair Regen. 23 (4) (2015) 465–482, https://doi.org/10.1111/wrr.12304.
[48] M.N.M. Walter, K.T. Wright, H.R. Fuller, S. MacNeil, W.E.B. Johnson, Mesenchymal stem cell-conditioned medium accelerates skin wound healing: an in vitro study of fibroblast and keratinocyte scratch assays, Exp. Cell Res. 316 (7) (2010) 1271–1281, https://doi.org/10.1016/j.yexcr.2010.02.026.
[49] Y. Cao, J. Yan, H. Liu, Clinical research progress of mesenchymal stem cells in treatment of chronic wounds, Chin. J. Reparative Reconstr. Surg. 35 (4) (2021) 496–501, https://doi.org/10.7507/1002-1892.202011009.